Journal of Engineering Mathematics **40:** 59–75, 2001.

Modelling of tension in yarn package unwinding

J.D. CLARK, W.B. FRASER* and D.M. STUMP[1]
School of Mathematics and Statistics, The University of Sydney NSW 2006, Australia
[1]*Department of Mathematics, The University of Queensland, St. Lucia, QLD 4072, Australia*
**Author for correspondence*

Received 21 October 1999; accepted in revised form 6 March 2000

Abstract. An improved theory for the variation of yarn tension during high speed over-end unwinding from cylindrical yarn packages based upon the theory of bent and twisted elastic rods is presented. A singular perturbation analysis is used to show that the effects of bending and twisting stiffnesses are confined to a boundary layer in the neighbourhood of the unwind point while, over most of the yarn path, the yarn motion can be analysed with a string theory. The boundary-layer analysis provides a description for the cohesive forces that hold the yarn windings in the package.

In most situations the motion of the unwind point forwards and backwards over the package is much longer than the rotational time of the balloon about the package axis, and a two-timing analysis is used to simulate this process as a series of quasi-stationary yarn balloons. The motion of the unwind point is shown to be asymmetrical with respect to its direction of motion on the package surface, which is in qualitative agreement with experimental measurements.

Key words: yarn balloons, yarn package unwinding, boundary layers, matched asymptotic expansions, two-timing analysis

1. Introduction

Over-end unwinding of yarn from large helically wound cylindrical packages is fundamental to many operations in the textile industry. In this process the package is held stationary and the yarn is withdrawn at a high constant speed $\mathcal{V}$ through a *guide-eye* located at a fixed point on the package axis ($\mathcal{V}$ in Figure 1). The loop of yarn *OPL* between the guide-eye and the package attains a considerable angular velocity about the package axis and the imaginary surface generated by this rotating loop is called a *balloon.* Yarn balloons also occur in other yarn transport and manufacturing processes such as ring-spinning and two-for-one twisting.

The theory of yarn balloon formation is thus of significant interest to the textile industry and a considerable literature exists. References [1]–[5] provide a more complete discussion of the development of the theory and earlier literature on the unwinding balloon, while [6] provides a comprehensive list of references to the literature on ring-spinning and two-for-one twister balloons. The investigation described in this paper extends the work reported in the papers by Padfield [1], Kothari and Leaf [2], and Fraser *et al.* [3].

The purpose of the present investigation is to give a complete analysis of the motion of the yarn between the *unwind point U*, where the yarn first moves from its stationary position on the package surface, and the guide-eye *O.* At the *lift-off* point *L* the yarn leaves the package surface and flies into the balloon. Over most of its path from *U* to *O* the yarn can be modelled as a perfectly flexible string, and this is the model used in the papers already mentioned. In the paper by Fraser *et al.* [3] two-timing asymptotics [7, pp. 37–117] are used to simulate

the unwinding process as a sequence of *quasi-stationary* balloons as the unwind point U is stepped uniformly backwards and forwards along the package surface. This asymptotic expansion is based on the assumption that the *wind-on* angle ϕ_u, is small. Although the results obtained under this assumption explained most of the yarn tension variation at the guide-eye during unwinding, recent experimental work by Kong *et al.* [8] reveals a number of significant difficulties with that model:

1. The experimental tension results exhibit a distinct asymmetry with respect to whether point U is moving away from, or towards the guide-eye. That is, with respect to the sign of the wind-on angle ϕ_u. ($\phi_u > 0$ when U moves away from the guide-eye, and $\phi_u < 0$ when it moves towards the guide-eye.) The simulations reported in [3] showed a symmetrical guide-eye tension variation as the point U moved backwards and forwards along the package surface.
2. There is clear experimental evidence that in the neighbourhood of U the curvature of the yarn varies rapidly enough so that in a flexible string model the yarn path would have a kink at U. In this paper the yarn is modelled as a uniform elastic rod of circular cross-section and small bending and torsional stiffnesses B and K respectively. It is clear that over most of the yarn path between U and O these stiffnesses can be neglected and the flexible string is a satisfactory model. However, in the neighbourhood of the unwind-point U there is a bending boundary-layer in which bending stiffness becomes significant for the determination of the yarn path near U. This boundary-layer analysis also provides a model for the cohesive force that holds the yarn in the package.

In the next section the derivation of the elastic-rod yarn model is reviewed. The equations are then recast into a suitable dimensionless form that reflects the fact that the cross-sectional radius of the yarn is very small compared with the package radius. In Section 3 a singular perturbation analysis is used to develop the $O(1)$ equations for the yarn path in the outer region away from the unwind point U, and in the boundary-layer in the neighbourhood of U. This formally justifies the use of a string theory to model the balloon and provides a set of boundary conditions at the unwind point U. In Section 4, a two-timing analysis is applied to the $O(1)$ equations obtained from the singular perturbation analysis to show that the unwinding process can be modelled as a set of quasi-stationary problems as the unwind point moves backwards and forwards along the package surface. This also explains the asymmetry observed in the experimental results. Section 5 presents a set of numerical calculations to simulate the unwinding problem.

2. The mathematical formulation

In this paper the yarn is modelled as an elastic rod of uniform circular cross-section radius a, mass per unit length m, and inextensible centre-line. The torque/torsion, and bending moment/curvature constitutive equations are assumed to be linear. The bending and torsional stiffnesses [9, pp. 162] are given by

$$K = \tfrac{1}{2}GAa^2, \text{ and } B = \tfrac{1}{4}EAa^2, \tag{2.1}$$

where: E is the Young's modulus; G is the shear modulus; and $A = \pi a^2$ is the cross-sectional area of the rod. If ν is Poisson's ratio then $G = E/[2(1+\nu)]$, and with $\nu = 0{\cdot}5$ (the incompressible limit) this leads to

$$K = \tfrac{2}{3}B. \tag{2.2}$$

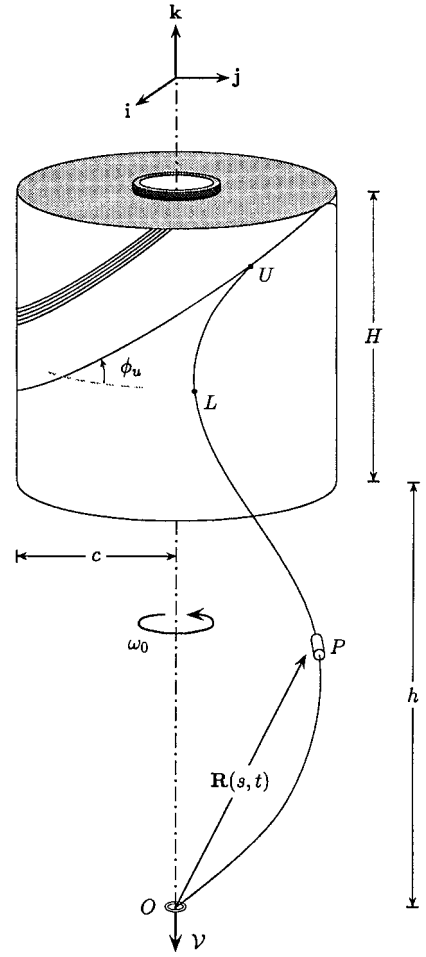

Figure 1. Schematic diagram of the over-end unwinding process: guide-eye *O*; balloon *OPL*; lift-off point *L*; unwind point *U*; wind-on angle ϕ_u; withdrawl speed $\mathcal{V}$.

The point to be made here is that these stiffnesses have the same order of magnitude. These formulae are also used below to estimate this order of magnitude.

Figures 2a and 2b show the forces and moments acting on a material element of the yarn at *P* which has position vector $\mathbf{R}(s, t)$ relative to the origin *O* of a Cartesian coordinate system $Oxyz$ (with base vectors **i**, **j**, **k**) that rotates with constant angular velocity $\omega_0\mathbf{k}$ about the axis of the cylindrical package (Figure 1). Here *s* is the distance of *P* along the yarn from *O* at time *t*. Note that in this problem ω_0 is the average angular speed of the unwinding balloon taken over the unwinding cycle as the unwind point *U* moves from the front (nearest the guide-eye *O*) to the rear of the package and back. This speed must be determined as part of the solution of the problem as a function of the wind-on angle ϕ_u and the unwinding speed $\mathcal{V}$.

Equations for the rate of change of linear and angular momentum of the right cylindrical yarn element with its centre of mass located at *P* will now be derived.

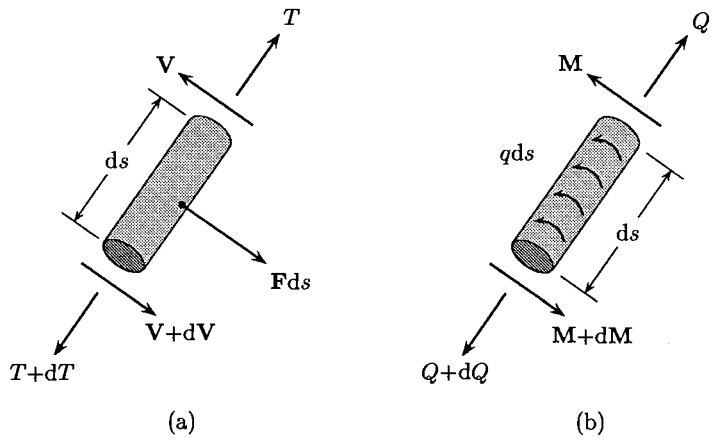

Figure 2. (a) Forces acting on the cylindrical yarn element *P.* Shear force **V** perpendicular to the yarn tangent vector, yarn tension T, and frictional or air drag force **F** per unit length. (b) Moment vectors acting on the cylindrical yarn element at *P.* Axial torque Q, bending moment **M**, and axial torque generated by surface friction forces q per unit length.

2.1. LINEAR MOMENTUM

The equation for the rate of change of linear momentum is

$$m\left\{D^2\mathbf{R} + 2\omega_0\mathbf{k} \times D\mathbf{R} + \omega_0^2\mathbf{k} \times (\mathbf{k} \times \mathbf{R})\right\} = (T\mathbf{R}')' + \mathbf{V}' + \mathbf{F}, \tag{2.3}$$

where: $(\,)' = \partial(\,)/\partial s$; and $T(s, t)$ is the tension in the yarn. The shear force **V** acts on the cross section perpendicular to the yarn axis. This force is present because the bending stiffness of the yarn is now taken into consideration. For a flexible yarn $\mathbf{V} = \mathbf{0}$ everywhere. The operator D is the material derivative, relative to the rotating coordinate system, following the motion of the yarn element P through the balloon:

$$D = \frac{\partial}{\partial t} - \mathcal{V}\frac{\partial}{\partial s}, \tag{2.4}$$

and $\mathcal{V}$ is the (constant) speed of the yarn through the balloon.

The vector **F** is the force per unit length on the yarn due to frictional drag if the yarn is moving in contact with the surface of the package or due to air-drag when the yarn is in the balloon. The air drag, acting on a freely ballooning yarn, is assumed to act in the opposite direction to the component $\mathbf{v}_n$, of the yarn velocity normal to the yarn axis, and to have a magnitude proportional to $|\mathbf{v}_n|^2$. The equation for the air drag is

$$\left.\begin{aligned} \mathbf{F} &= -D_n|\mathbf{v}_n|\mathbf{v}_n, \\ \text{where } \mathbf{v}_n &= \mathbf{v} - (\mathbf{v}\cdot\mathbf{R}')\mathbf{R}', \\ \text{and } \mathbf{v} &= D\mathbf{R} + \omega_0\mathbf{k} \times \mathbf{R} \end{aligned}\right\} \tag{2.5}$$

is the yarn velocity relative to an inertial reference frame, and D_n, is the air-drag coefficient [3].

The total force that the package exerts on the yarn is given by

$$\mathbf{F} = N\mathbf{e}_r - \mu N\frac{\mathbf{v}}{|\mathbf{v}|}, \tag{2.6}$$

where: ($\mathbf{e}_r$, $\mathbf{e}_\theta$, $\mathbf{k}$) are the basis vectors of the cylindrical coordinate system r, θ, z relative to the rotating Cartesian coordinate system; N is the normal force between the yarn and the package; and μ is the coefficient of sliding friction.

The inextensibility condition is

$$\frac{\partial \mathbf{R}}{\partial s} \cdot \frac{\partial \mathbf{R}}{\partial s} = 1. \tag{2.7}$$

2.2. Angular momentum

The yarn is modelled as a linearly elastic inextensible rod of uniform circular cross-section deforming under the Kirchhoff hypothesis that plane sections remain plane, undeformed, and perpendicular to the rod axis (see [10] for details).

The moment of inertia of the right-cylindrical element is the same about all diameters, and the principal moments of inertia of the element of length δs are $I_1 = 1/2(ma^2\delta s)$, $I_2 = I_3 = 1/4(ma^2\delta s)$ with respect to the orthogonal material axes ($\mathbf{R}'$, $\mathbf{d}_2$, $\mathbf{d}_3$) where $\mathbf{d}_2$ and $\mathbf{d}_3$ are embedded within the material cross section and where $\mathbf{R}' = \mathbf{d}_2 \times \mathbf{d}_3$. The angular velocity $\mathbf{\Omega}$ of the element is given by

$$\mathbf{\Omega} = \omega_t \mathbf{R}' + \mathbf{R}' \times (D\mathbf{R}' + \omega_0 \mathbf{k} \times \mathbf{R}'), \tag{2.8}$$

and the angular momentum vector relative to the centre of mass of the element is therefore given by

$$\mathbf{H}\delta s = \tfrac{1}{2} ma^2 \delta s \left\{ \omega_t \mathbf{R}' + \tfrac{1}{2} [\mathbf{R}' \times (D\mathbf{R}' + \omega_0 \mathbf{k} \times \mathbf{R}')] \right\}, \tag{2.9}$$

where $\omega_t \mathbf{R}'$ is the component of the angular velocity of the yarn element about the yarn axis. The equation for the rate of change of angular momentum of the mass element expressed in the reference frame which spins with the angular velocity $\omega_0 \mathbf{k}$ is

$$\begin{aligned} D\mathbf{H} + \omega_0 \mathbf{k} \times \mathbf{H} &= \tfrac{1}{2} ma^2 \left\{ D(\omega_t \mathbf{R}') + \tfrac{1}{2} \mathbf{R}' \times D^2 \mathbf{R}' - \omega_0 (\mathbf{k} \cdot \mathbf{R}') D\mathbf{R}' \right. \\ &\quad \left. + \tfrac{1}{2} \omega_0 (2\omega_t - \omega_0 \mathbf{k} \cdot \mathbf{R}')(\mathbf{k} \times \mathbf{R}') \right\} \\ &= (Q\mathbf{R}')' + \mathbf{M}' + \mathbf{R}' \times \mathbf{V} + q\mathbf{R}', \end{aligned} \tag{2.10}$$

where: $Q\mathbf{R}'$ is the axial torque vector; $\mathbf{M}$ is the bending moment vector; and $q\mathbf{R}'$ is the axial moment per unit yarn length due to frictional forces exerted on the surface of the yarn moving on the package surface between unwind-point U and the lift-off point L in Figure 1. On the assumption of Amonton's law

$$q = a\mu N, \tag{2.11}$$

where μ and N are defined in Equation (2.6). For a freely ballooning yarn $q = 0$.

These equations are supplemented with the inextensibility constraint Equation (2.7), along with the normality constraints

$$\mathbf{V} \cdot \mathbf{R}' = 0 \quad \text{and} \quad \mathbf{M} \cdot \mathbf{R}' = 0. \tag{2.12}$$

The moment-curvature and torque-torsion constitutive relations are

$$\mathbf{M} = B(\mathbf{R}' \times \mathbf{R}'') \quad \text{and} \quad Q = K(\phi' - \mathbf{b}' \cdot \mathbf{n}), \tag{2.13}$$

where the *torsion* $(\phi' - \mathbf{b}' \cdot \mathbf{n})$ is the sum of the *twist* ϕ' and the *tortuosity* of the yarn path $-\mathbf{b}' \cdot \mathbf{n}$ of Love [11, pp. 381–396]. (Here $\mathbf{n}$ and $\mathbf{b}$ are the normal and binormal vectors of the yarn path.)

2.2.1. *The twist flow equation*

To complete the formulation of the problem an equation governing the flow of twist along the yarn must be added to the dynamic equations. The derivation of this equation is given in [10].

Let $\mathcal{N}(s, t)$ (radians) be the total angular rotation undergone by the yarn cross section since it started moving from the unwind-point U in Figure 1. The torsion and the angular speed ω_t are related to this function as follows:

$$\frac{\partial \mathcal{N}}{\partial s} = (\phi' - \mathbf{b}' \cdot \mathbf{n}) \quad \text{and} \quad D\mathcal{N} = \omega_t. \tag{2.14}$$

Note, the difference in the definition of ω_t between this paper and [10] is that ω_t defined here includes the term $(\mathbf{k} \cdot \mathbf{R}')\omega_0$. Also the definition of $\mathcal{N}(s, t)$ as the integral of the torsion given in that paper is only valid for *quasi-stationary* balloons that are independent of time when viewed from the rotating reference frame.

2.3. Dimensionless equations

Dimensionless (barred) variables are defined as follows:

$$\begin{aligned} &\bar{\mathbf{R}} = \frac{\mathbf{R}}{c}, \quad \bar{s} = \frac{s}{c}, \quad \bar{\mathbf{v}} = \frac{\mathbf{v}}{\omega_0 c}, \quad \bar{\mathcal{V}} = \frac{\mathcal{V}}{\omega_0 c}, \quad \bar{t} = \omega_0 t, \\ &\bar{D} = \frac{\partial}{\partial t} - \mathcal{V}\frac{\partial}{\partial \bar{s}}, \quad \bar{T} = \frac{T}{m\omega_0^2 c^2}, \quad \bar{N} = \frac{N}{m\omega_0^2 c^2}, \quad \bar{\mathbf{F}} = \frac{\mathbf{F}}{m\omega_0^2 c^2}. \end{aligned} \tag{2.15}$$

The dimensionless moment, shear force and yarn twist variables are:

$$\begin{aligned} &\bar{\mathbf{H}} = \frac{\mathbf{H}}{m\omega_0 c^2}, \quad \bar{\mathbf{V}} = \frac{\mathbf{V}}{m\omega_0^2 c^2}, \quad \bar{\mathbf{M}} = \frac{\mathbf{M}}{m\omega_0^2 c^3}, \\ &\bar{Q} = \frac{Q}{m\omega_0^2 c^3}, \quad \bar{q} = \frac{q}{m\omega_0^2 c^2} = \delta\mu\bar{N}, \end{aligned} \tag{2.16}$$

where $\delta = a/c$, and the angular velocities have been scaled against the average angular speed of the balloon ω_0.

As all variables will be dimensionless from now on, unless specifically stated otherwise, the barred notation will be dropped.

The dimensionless form of the rate of change of linear momentum Equation (2.3) is

$$D^2\mathbf{R} + 2\mathbf{k} \times D\mathbf{R} + \mathbf{k} \times (\mathbf{k} \times \mathbf{R}) = (T\mathbf{R}')' + \mathbf{V}' + \mathbf{F}, \tag{2.17}$$

where in the freely ballooning yarn the air-drag $\mathbf{F} = -(p_0/16)|\mathbf{v}_n|\mathbf{v}_n$, and on the package $\mathbf{F}$ is still given by Equation (2.6). The dimensionless air-drag coefficient $p_0 = 16cD_n/m$ introduced in [1] takes on values between 2 and 4 for typical yarns.

The rate of change of the angular momentum Equation (2.10) is now given by

$$\begin{aligned} D\mathbf{H} + \mathbf{k} \times H \;&=\; \tfrac{1}{2}\delta^2 \left\{ D(\omega_t \mathbf{R}') + \tfrac{1}{2}\mathbf{R}' \times D^2\mathbf{R}' - (\mathbf{k} \cdot \mathbf{R}')D\mathbf{R}' \right. \\ &\qquad \left. + \tfrac{1}{2}(2\omega_t - \mathbf{k} \cdot \mathbf{R}')(\mathbf{k} \times \mathbf{R}') \right\} \\ &=\; (Q\mathbf{R}')' + \mathbf{M}' + \mathbf{R}' \times \mathbf{V} + q\mathbf{R}'. \end{aligned} \tag{2.18}$$

The dimensionless constitutive equations are

$$\mathbf{M} = \beta\frac{\delta^2}{\gamma}(\mathbf{R}' \times \mathbf{R}'') \quad \text{and} \quad Q = \kappa\frac{\delta^2}{\gamma}(\phi' - \mathbf{b}' \cdot \mathbf{n}), \tag{2.19}$$

where

$$\delta = \frac{a}{c} \approx 10^{-3} \quad \text{and} \quad \gamma = \frac{m\omega_0^2 c^2}{EA} \approx 10^{-3}. \tag{2.20}$$

γ is the elasticity parameter introduced in [4]. For an isotropic linear elastic rod with Poisson's ratio ν

$$\beta = \frac{1}{4} \quad \text{and} \quad \kappa = \frac{1}{(1+\nu)} \tag{2.21}$$

are both $O(1)$ quantities.

The rotation satisfies a wave equation found as follows. First, form the scalar product of Equation (2.18) with $\mathbf{R}'$ to obtain

$$\tfrac{1}{2}\delta^2 D\omega_t = Q' + q, \tag{2.22}$$

where $q = 0$ in the freely ballooning yarn between O and L and $q = \delta\mu N$ between L and U. When use is made of the definition of the rotation $\mathcal{N}(s,t)$, Equations (2.14), in the above equation the result is

$$\tfrac{1}{2}D^2\mathcal{N} = \frac{\kappa}{\gamma}\mathcal{N}'', \tag{2.23}$$

in the freely ballooning yarn. Finally, if Equation (2.22) is subtracted from Equation (2.18) the equation for the component of the rate of change of angular momentum transverse to the yarn axis is obtained:

$$\begin{aligned}&\tfrac{1}{2}\delta^2\left\{(\mathbf{R}' \times D^2\mathbf{R}') + (\omega_t - \mathbf{k}\cdot\mathbf{R}')D\mathbf{R}' + \tfrac{1}{2}(2\omega_t - \mathbf{k}\cdot\mathbf{R}')(\mathbf{k}\times\mathbf{R}')\right\}\\ &= Q\mathbf{R}'' + \mathbf{M}' + \mathbf{R}' \times \mathbf{V}.\end{aligned} \tag{2.24}$$

The geometric boundary conditions that apply to these equations for the yarn unwinding problem are straight forward: at the guide-eye O where $s = 0$ and at the lift-off point L where $s = s_\ell$. They are:

$$\mathbf{R}(0,t) = 0 \quad \text{and} \quad \mathbf{R}(s_\ell,t)\cdot\mathbf{e}_r = 1, \quad \mathbf{R}'(s_\ell,t)\cdot\mathbf{e}_r = 0, \tag{2.25}$$

that is, at the lift-off point, the yarn just touches the package surface and its tangent is continuous and lies in the tangent plane to the package surface. In addition, the position, tangent and velocity vectors are continuous at s_ℓ.

The boundary conditions at the unwind-point U, however, are more complicated, because this point moves up and down the package as the yarn is unwound, and at this point the yarn begins to move from its stationary position on the package surface. (The development of the boundary condition at U is deferred until Section 3.2 below.)

Examination of the dimensionless Equations (2.17), (2.20) and (2.24) suggests that, since δ^2 is very small and γ is also small, over most of the yarn path where the curvature is small the

effect of angular momentum, bending moment, torque and transverse shear can be neglected. Thus, over most of the yarn path $\mathbf{M} = \mathbf{V} = \mathbf{0}$, and the motion is governed by the linear momentum equation alone. However, in the neighbourhood of U the yarn can undergo a distinct kink or rapid change in the direction of its tangent vector, as observed experimentally in [8], and these quantities can not be ignored. In the next section a boundary layer solution, valid in the neighbourhood of U, is constructed and solution of this boundary layer problem provides the boundary condition at U. This will now be established by a singular perturbation analysis.

3. Perturbation analysis

Since this is a bending boundary-layer problem, the appropriate small parameter for the perturbation expansions is

$$\epsilon^2 = \frac{\delta^2}{\gamma} \approx 10^{-3}, \tag{3.1}$$

which compares with the small parameter defined for the bending boundary layer in the moving strip problem [12]. From Equation (2.20) it can also be deduced that $O(\delta) \sim O(\epsilon^2)$. It will thus be convenient to write

$$\delta = \alpha\epsilon^2, \tag{3.2}$$

where α is an $O(1)$ parameter.

3.1. The outer expansion

Over most of the yarn path between O and U, except in the neighbourhood of U, expansions of the form

$$\left.\begin{aligned} T(s,t) &= T_0(s,t) + \epsilon T_1(s,t) + \epsilon^2 T_2(s,t) + \cdots, \\ \mathbf{R}(s,t) &= \mathbf{R}_0(s,t) + \epsilon\mathbf{R}_1(s,t) + \epsilon^2\mathbf{R}_2(s,t) + \cdots \end{aligned}\right\} \tag{3.3}$$

and so on are substituted into the dimensionless equations to obtain a hierarchy of problems in powers of ϵ.

The separated constitutive Equations (2.19) give the immediate results

$$\left.\begin{aligned} &\mathbf{M}_0 = \mathbf{M}_1 = 0, \quad \mathbf{M}_2 = \beta(\mathbf{R}_0' \times \mathbf{R}_0''), \\ &Q_0 = Q_1 = 0, \quad Q_2 = \kappa(\phi_0' - \mathbf{b}_0' \cdot \mathbf{n}_0), \end{aligned}\right\} \tag{3.4}$$

while the angular momentum Equation (2.24) becomes

$$\begin{aligned} &\tfrac{1}{2}\alpha^2\epsilon^4 \left\{ \tfrac{1}{2}(\mathbf{R}_0 \times D^2\mathbf{R}_0') + (\omega_{t0} - \mathbf{k}\cdot\mathbf{R}_0')D\mathbf{R}_0' + \tfrac{1}{2}(2\omega_{t0} - \mathbf{k}\cdot\mathbf{R}_0')(\mathbf{k}\times\mathbf{R}_0) \right\} \\ &\qquad = \epsilon^2[Q_2\mathbf{R}_0'' + \mathbf{M}_2'] + (\mathbf{R}_0' + \epsilon\mathbf{R}_1' + \epsilon^2\mathbf{R}_2') \times (\mathbf{V}_0 + \epsilon\mathbf{V}_1 + \epsilon^2\mathbf{V}_2). \end{aligned} \tag{3.5}$$

It follows from this equation that

$$\mathbf{V}_0 = \mathbf{V}_1 = \mathbf{0},$$

and

$$Q_2\mathbf{R}_0'' + \mathbf{M}_2' + \mathbf{R}_0' \times \mathbf{V}_2 = \mathbf{0}. \tag{3.6}$$

Thus, yarn twist and bending stiffnesses have at most an $O(\epsilon^2)$ effect on the yarn path except near the unwind point U where the derivatives $\mathbf{R}''$ and $\mathbf{R}'''$ may become large. This means that to this order the yarn path is determined by the linear momentum Equation (2.17) which, to $O(1)$, becomes

$$D^2\mathbf{R}_0 + 2\mathbf{k} \times D\mathbf{R}_0 + \mathbf{k} \times (\mathbf{k} \times \mathbf{R}_0) = (T_0\mathbf{R}_0')' + \mathbf{F}_0. \tag{3.7}$$

This result agrees with the comparable expression obtained in [10] for the ring-spinning balloon.

The detailed solution of this equation will be described in Section 4 after the boundary-layer expansion has been discussed.

3.2. The boundary-layer expansion

In the boundary layer at U the following coordinate and variable transformations are introduced:

$$\eta = \frac{s_u(t) - s}{\epsilon}, \quad \mathbf{R}(s, t) = \mathbf{R}_u(t) + \epsilon\hat{\mathbf{r}}(\eta, t), \tag{3.8}$$

where $s_u(t)$ is the length of yarn between O and U at time t, and $\mathbf{R}_u(t)$ is the position vector of U, a function of time alone:

$$\frac{\mathrm{d}\mathbf{R}_u}{\mathrm{d}t} + \mathbf{e}_\theta = (\dot{s}_u(t) + \mathcal{V})(\cos\phi_u\mathbf{e}_\theta + \sin\phi_u\mathbf{k}), \tag{3.9}$$

where $\dot{s}_u = \mathrm{d}s_u/\mathrm{d}t$, and at U, $\eta = 0$ and $\hat{\mathbf{r}} = \mathbf{0}$. From now on boundary layer variables will be distinguished with a hat.

The operators D and D_2 transform to

$$\left.\begin{aligned} D &= \frac{\partial}{\partial t} + \frac{1}{\epsilon}(\dot{s}_u + \mathcal{V})\frac{\partial}{\partial\eta}, \\ D^2 &= \frac{\partial^2}{\partial t^2} + \frac{\ddot{s}_u}{\epsilon}\frac{\partial}{\partial\eta} + \frac{2}{\epsilon}(\dot{s}_u + \mathcal{V})\frac{\partial^2}{\partial t\,\partial\eta} + \frac{1}{\epsilon^2}(\dot{s}_u + \mathcal{V})^2\frac{\partial^2}{\partial\eta^{2\cdot}} \end{aligned}\right\} \tag{3.10}$$

The constitutive Equations (2.19) transform into

$$\hat{\mathbf{M}} = -\epsilon\beta(\hat{\mathbf{r}}_\eta \times \hat{\mathbf{r}}_{\eta\eta}), \quad \hat{Q} = -\epsilon\kappa(\hat{\phi}_\eta - \mathbf{b}_\eta \cdot \mathbf{n}), \tag{3.11}$$

where $(\,)_\eta = \partial(\,)\partial\eta$.

In order to facilitate the solution of the boundary-layer equations, a local coordinate system of unit orthogonal basis vectors with its origin at U is introduced:

$$\left.\begin{aligned} \mathbf{e}_1 &= -\cos\phi_u\mathbf{e}_\theta - \sin\phi_u\mathbf{k}, \\ \mathbf{e}_2 &= \sin\phi_u\mathbf{e}_\theta - \cos\phi_u\mathbf{k}, \end{aligned}\right\} \tag{3.12}$$

which lie in the tangent plane to the package surface at U, see Figure 3. (Note also that $\mathbf{e}_1 \times \mathbf{e}_2 = \mathbf{e}_r$.)

As discussed in [12], the remote inner solution must approach a straight line as $\eta \to \infty$ in order that $\hat{\mathbf{M}}$ and $\hat{\mathbf{V}} \to \mathbf{0}$ and the remote tension $\hat{T}$ in the strand matches with that in the

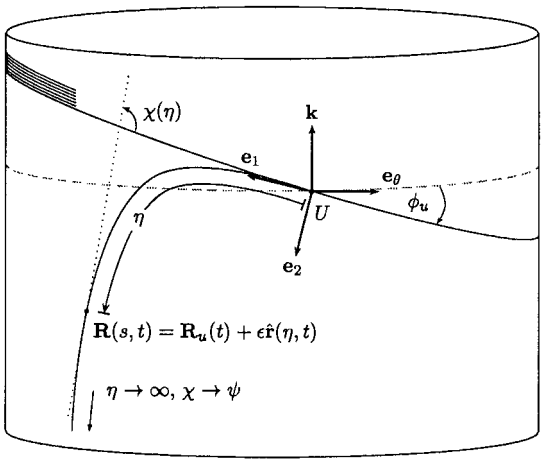

Figure 3. The coordinate system describing the boundary layer at the unwind point U. $\phi_u > 0$ as U moves away from the guide eye (forward unwinding), and $\phi_u < 0$ as U moves toward the guide eye (backward unwinding).

outer solution. Thus, the boundary cnndition on $\hat{\mathbf{r}}(\eta)$ at U is $\hat{\mathbf{r}}(0) = \mathbf{0}$, and as $(\eta \to \infty)$ the boundary conditions are determined by the matching conditions between the inner and outer solutions:

$$\left.\begin{aligned} \lim_{\eta\to\infty} \mathbf{R}_u(t) + \epsilon\hat{\mathbf{r}}(\eta, t) &= \lim_{s\to s_u} \mathrm{R}(s, t), \\ \lim_{\eta\to\infty} \hat{\mathbf{r}}_\eta(\eta, t) &= \lim_{s\to s_u} \mathrm{R}'(s, t), \\ \lim_{\eta\to\infty} \hat{T}(\eta, t) &= \lim_{s\to s_u} T(s, t), \\ \lim_{\eta\to\infty} \hat{\mathbf{M}}(\eta, t) = \hat{\mathbf{V}}(\eta, t) &= \mathbf{0} \end{aligned}\right\} \tag{3.13}$$

where $\mathbf{R}(s, t)$ and $T(s, t)$ are outer solution quantities.

The boundary-layer variables are now expanded in power series:

$$\left.\begin{aligned} \hat{\mathbf{r}} &= \hat{\mathbf{r}}_0 + \epsilon\hat{\mathbf{r}}_1 + \epsilon^2\hat{\mathbf{r}}_2 + \cdots, \\ \hat{\mathbf{V}} &= \hat{\mathbf{V}}_0 + \epsilon\hat{\mathbf{V}}_1 + \epsilon^2\hat{\mathbf{V}}_2 + \cdots, \end{aligned}\right\} \tag{3.14}$$

and so on, and these are substituted into the transformed governing equations to obtain a hierarchy of equations in powers of ϵ.

From Equation (2.22) it is found that $\hat{Q}_0 = 0$ and $\hat{Q}_{1\eta} = 0$, and the $O(1)$ result from the angular momentum Equation (2.24) is

$$\beta(\hat{\mathbf{r}}_{0\eta} \times \hat{\mathbf{r}}_{0\eta\eta})_\eta - \hat{\mathbf{r}}_{0\eta} \times \hat{\mathbf{V}}_0 = \mathbf{0}. \tag{3.15}$$

The $O(1/\epsilon)$ term of linear momentum Equation (2.17) is

$$(\dot{s}_{u0} + \mathcal{V})^2\hat{\mathbf{r}}_{0\eta\eta} = (\hat{T}'\hat{\mathbf{r}}_{0\eta})_\eta - \hat{\mathbf{V}}_{0\eta}. \tag{3.16}$$

Notice that $\hat{N}$, the normal force per unit arc-length, which is perpendicular to the package surface, drops out at this order so that the boundary layer is tangent to the package surface and

lies in a plane spanned by the $\mathbf{e}_\theta$ and $\mathbf{k}$ directions. Now express $\hat{\mathbf{r}}_{0\eta}$ in terms of the angle $\chi(\eta)$ between the yarn tangent vector and $\mathbf{e}_1$, so that

$$\hat{\mathbf{r}}_{0\eta} = \cos\chi\,\mathbf{e}_1 + \sin\chi\,\mathbf{e}_2. \tag{3.17}$$

In order to obtain the differential equation for χ proceed as follows. First, Equation (3.16) is integrated to obtain

$$(\dot{s}_{u0} + \mathcal{V})^2\hat{\mathbf{r}}_{0\eta} = \hat{T}_0\hat{\mathbf{r}}_{0\eta} - \hat{\mathbf{V}}_0 + \mathbf{C}, \tag{3.18}$$

where $\mathbf{C}$ is a constant of integration, which is found from the matching conditions Equation (3.13) to be

$$\mathbf{C} = [(\dot{s}_{u0} + \mathcal{V})^2 - T_0(s_{u0}, t)](\cos\psi_0\mathbf{e}_1 + \sin\psi_0\mathbf{e}_2).$$

T_0 and ψ_0 are determined from the outer solution, and, to O(1), matching condition Equation $(3.13)_2$ gives $\lim_{\eta\to\infty}\chi \to \psi_0$. Note that $\chi_\eta, \chi_{\eta\eta}, \ldots$ all tend to zero as $\eta \to \infty$. Next, the scalar product of Equation (3.18) with $\hat{\mathbf{e}}_{0\eta}$ is formed to give

$$\hat{T}_0 = \left[T_0(s_{u0}, t) - (\dot{s}_{u0} + \mathcal{V})^2\right]\cos(\psi_0 - \chi) + (\dot{s}_{u0} + \mathcal{V})^2. \tag{3.19}$$

The above results are substituted back into Equation (3.18) to obtain the shear force expression

$$\hat{\mathbf{V}}_0 = [T_0(s_{u0}, t) - (\dot{s}_{u0} + \mathcal{V})^2]\sin(\psi_0 - \chi)(\sin\chi\,\mathbf{e}_1 - \cos\chi\,\mathbf{e}_2). \tag{3.20}$$

Second, the formation of the vector product of $\hat{\mathbf{r}}_{0\eta}$ with Equation (3.15), followed by the substitution of Equation (3.17) provides a further expression for $\hat{\mathbf{V}}_0$:

$$\hat{\mathbf{V}}_0 = -\beta\chi_{\eta\eta}(\sin\chi\,\mathbf{e}_1 - \cos\chi\,\mathbf{e}_2). \tag{3.21}$$

The elimination of $\hat{\mathbf{V}}_0$ from Equations (3.20) and (3.21) gives the equation for χ:

$$\chi_{\eta\eta} = -\Lambda\sin(\psi_0 - \chi), \tag{3.22}$$

where

$$\Lambda = \beta^{-1}\left[T_0(s_{u0}, t) - (\dot{s}_{u0} + \mathcal{V})^2\right].$$

The first integral of this equation is

$$\left(\frac{\mathrm{d}\chi}{\mathrm{d}\eta}\right)^2 = 2\Lambda\left[1 - \cos(\psi_0 - \chi)\right],$$

where the constant of integration has been determined from the matching conditions given above. A further integration leads to

$$\sqrt{\Lambda}\eta = \int_0^\chi \csc\left[\frac{1}{2}(\psi_0 - \chi')\right]\mathrm{d}\chi' = -\frac{1}{2}\ln\left[\tan\left(\frac{\psi_0 - \chi'}{4}\right)\right]\Bigg|_0^\chi,$$

which, on rearrangement, gives the final result

$$\chi(\eta) = \psi_0 - 4\arctan\left[\left(\tan\frac{\psi_0}{4}\right)e^{-\sqrt{\Lambda}\eta}\right]. \tag{3.23}$$

Thus, once ψ_0 and $\dot{s}_{u0}(t)$ are known $\chi(\eta)$ is completely determined, and hence the $O(1)$ tension and shear force in the boundary layer are then determined from Equations (3.19) and (3.20).

The tension and shear force at the unwind point are given respectively by the quantities $\hat{T}_0(0)$ and $\hat{\mathbf{V}}_0(0)$. In order to model the motion of the unwind point it is necessary to postulate a physical mechanism which initiates yarn movement along the package surface. Since the yarn elements are constrained to move in a direction perpendicular to the stationary windings, and since the tension in an inextensible yarn is determined entirely by the yarn dynamics between O and U (and can not be specified at U), the cohesive forces that hold the yarn in the package are modelled by setting the magnitude of the shear force $|\hat{\mathbf{V}}_0(0)|$ at the end of the boundary layer equal to a critical package parameter V_c:

$$V_c = \left|\left[T_0(s_{u0}, t) - (\dot{s}_{u0} + \mathcal{V})^2\right] \sin\psi_0\right| . \tag{3.24}$$

4. The two-timing analysis

To complete the analysis of package unwinding, it is necessary to consider the motion of the unwind point backwards and forwards along the package through a single unwinding cycle. If the wind-on angle ϕ_u is small ($|\phi_u| \leq 15°$) the period Γ of the cycle is much longer than the rotational timescale (ω_0^{-1}). On this slow timescale the motion of the yarn as U moves through one unwind cycle will be modelled as a series of decoupled quasi-static balloon shapes which are stationary when viewed from the rapidly rotating reference frame. First, the motion of the unwind-point U is analysed, followed by a two-timing analysis of the boundary-layer and outer solution equations.

4.1. The motion of the unwind point

The time dependent motion of the unwind point is governed by Equation (3.9) which has components

$$\frac{\mathrm{d}\theta_u}{\mathrm{d}t} + 1 = (\dot{s}_u + \mathcal{V})\cos\phi_u, \quad \frac{\mathrm{d}z_u}{\mathrm{d}t} = (\dot{s}_u + \mathcal{V})\sin\phi_u \tag{4.1}$$

where $(1, \theta_u, z_u)$ are the cylindrical coordinate components of the position of U.

In order to integrate these equations, certain assumptions are made regarding the variation of the wind-on angle ϕ_u in the construction of the package. It is assumed that ϕ_u has the form shown schematically in Figure 4a. As the unwind point moves away from the guide eye during the time interval $0 \leq t \leq t_1$, ϕ_u, is a positive constant, while as the unwind point moves back towards the guide eye during the time interval $t_1 \leq t \leq \Gamma$, ϕ_u is a negative constant. At the front and back edges of the package, ϕ_u makes a rapid change in sign as the windings reverse direction. The simultaneous variation in the balloon length over the course of one cycle of motion of the unwind point is shown schematically in Figure 4b. Note that it is experimentally observed [8] that $t_1 \leq \Gamma/2$.

At the end of an unwind cycle, the position vector $\mathbf{R}_u(t)$ in the rotating frame and the yarn length $s_u(t)$ have returned to their starting values. Thus, these two quantities satisfy the periodicity conditions

$$\mathbf{R}_u(t + \Gamma) = \mathbf{R}_u(t), \quad \text{and} \quad s_u(t + \Gamma) = s_u(t). \tag{4.2}$$

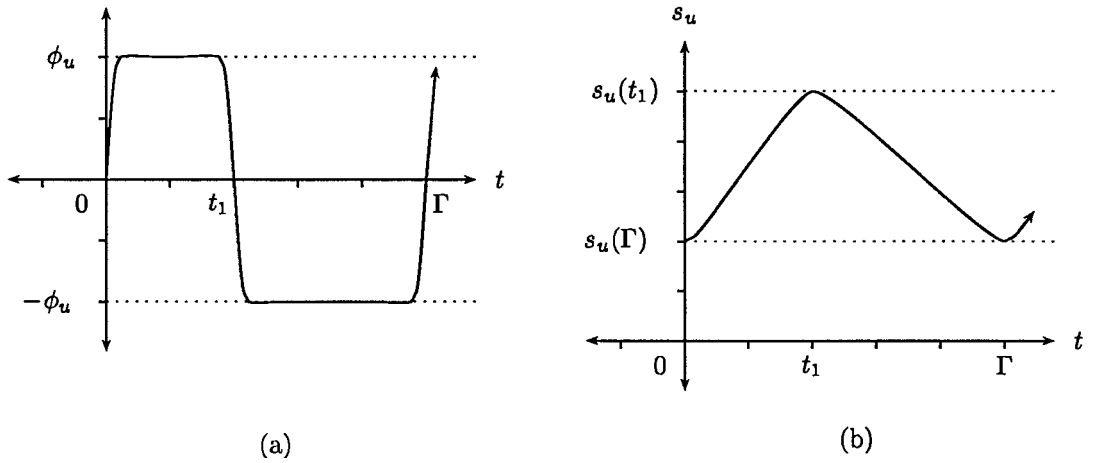

Figure 4. Schematic figures showing the variation in ϕ_u, (a), and s_u, (b), during one complete unwind cycle $0 \le t \le \Gamma$.

The component Equations (4.1) are integrated subject to the conditions

$$z_u(0) = z_u(\Gamma) = h, \quad z_u(t_1) = H + h, \quad \text{and} \quad \theta_u(0) = \theta_u(\Gamma) = 0$$

to obtain

$$\theta_u(t) - \theta_u(0) = -t + [s_u(t) - s_u(0) + \mathcal{V}t]\cos\phi_u, \quad 0 \le t \le \Gamma \tag{4.3}$$

and

$$z_u(t) - h = \begin{cases} [s_u(t) - s_u(0) + \mathcal{V}t]\sin|\phi_u|, & 0 \le t \le t_1, \\ -[s_u(t) - s_u(0) + \mathcal{V}(t-\Gamma)]\sin|\phi_u|, & t_1 \le t \le \Gamma \end{cases} \tag{4.4}$$

where, as indicated in Figure 1, the front of the package coincides with $z_u = h$ and the package height is H. The evaluation of Equation (4.3) at $t = \Gamma$ and Equation (4.4) at $t = t_1$ leads to the three relations

$$\frac{1}{\mathcal{V}} = \cos\phi_u, \quad s_u(t_1) - s_u(0) = \mathcal{V}\left(\frac{\Gamma}{2} - t_1\right), \quad \text{and} \quad \frac{2H}{\mathcal{V}\Gamma} = \sin\phi_u. \tag{4.5}$$

4.2. THE SLOW TIMESCALE

When the magnitude of the wind-on angle $|\phi_u|$ is small (i.e. $|\phi_u| \le 15°$), $\Gamma \gg \omega_0^{-1}$ and the concept of a slow timescale for the motion of the unwind point becomes meaningful. Thus, the unwind angle ϕ_u is rescaled as $\phi_u = \sigma\Phi_u$, where γ is a small parameter and Φ_u is an $O(1)$ quantity. This leads to the introduction of the 'slow' timescale variable

$$\tau = \sigma t.$$

The typical order of magnitude of σ is $O(10^{-1})$ [3]. This is somewhat larger than the parameter $\epsilon \sim O(\sqrt{10^{-3}})$ which enters into the boundary layer expansion, so that the spatial scale of the boundary layer is always small regardless of the position of the unwind point

during its periodic motion. Thus, the boundary-layer and outer solutions at any instant are reasonably approximated by the leading terms in the expansions developed in the previous section. From now on only the $O(1)$ equations from the boundary-layer and outer solutions given above will be used, *and the subscript zero on the variables in those equations will now be dropped.*

The equations that determine the outer solution are now rewritten in terms of the slow time τ. Explicit dependence on the fast timescale t is suppressed since the objective is to simulate the unwinding by a sequence of quasi-stationary balloon shapes. Equation (3.7) now becomes

$$\sigma^2\frac{\partial^2\mathbf{R}}{\partial\tau^2} - 2\sigma\mathcal{V}\frac{\partial\mathbf{R}'}{\partial\tau} + \mathcal{V}^2\mathbf{R}'' + 2\mathbf{k}\times\left(\sigma\frac{\partial\mathbf{R}}{\partial\tau} - \mathcal{V}\mathbf{R}'\right) + \mathbf{k}\times(\mathbf{k}\times\mathbf{R}) = (T\mathbf{R}')' + \mathbf{F}, \tag{4.6}$$

where $\mathbf{F}$ is given by the dimensionless form of Equation (2.5) between O and L, and by Equation (2.6) between L and U. This equation must be solved subject to the inextensibility condition $\mathbf{R}'\cdot\mathbf{R}' = 1$ and the boundary conditions: $\mathbf{R}(0,\tau) = 0$ at O; continuity of $\mathbf{R}'$, $\mathbf{R}$, and T at L where $s = s_\ell$; and the location of the unwind point U, the motion of which is governed by Equations (4.3) and (4.4). The rescaled critical shear force condition Equation (3.24) at the unwind point is

$$V_c = \left|\left[T(s_u,\tau) - (\sigma\dot{s}_u + \mathcal{V})^2\right]\sin\psi\right|, \tag{4.7}$$

where the $\dot{(\,)}$ now means differentiation with respect to τ.

All unknown variables $(\mathbf{R}, T, \mathbf{R}_u, s_u, \sigma\Gamma, \sigma t_1, \mathcal{V}, \psi)$ are now expanded as perturbation series in σ with the forms

$$\left.\begin{aligned} \mathbf{R}(s,\tau) &= \mathbf{R}_0(s) + \sigma\mathbf{R}_1(s,\tau) + \sigma^2\mathbf{R}_2(s,\tau) + \cdots, \\ \sigma\Gamma &= \Gamma_0 + \sigma\Gamma_1 + \sigma^2\Gamma_2 + \cdots \\ \sigma t_1 = \tau_1 &= \tilde{\tau}_0 + \sigma\tilde{\tau}_1 + \sigma^2\tilde{\tau}_2 + \cdots \end{aligned}\right\} \tag{4.8}$$

and so on. On the slow timescale the period $\sigma\Gamma$ and the half period $\tau_1 = \sigma t_1$ are $O(1)$ quantities. When these expansions are substituted into the rescaled forms of Equations (4.5), the following results are obtained:

$$\left.\begin{aligned} \mathcal{V} &= 1 + \sigma^2\frac{1}{2}\Phi_u^2 + \cdots, \\ \sigma\Gamma &= \frac{2H}{|\Phi_u|} - \sigma^2\frac{4H|\Phi_u|}{3} + \cdots, \\ \tau_1 &= \frac{H}{|\Phi_u|} - \sigma[s_{u0}(\tilde{\tau}_0) - s_{u0}(0)] + \cdots. \end{aligned}\right\} \tag{4.9}$$

These equations and the rescaled slow time $\tau = \sigma t$ are now used in Equation (4.3) and (4.4) to obtain the position of the unwind point as a function of τ:

$$\theta_{u0}(\tau) + \sigma\theta_{u1}(\tau) + \cdots = s_{u0}(\tau) - s_{u0}(0) + \sigma\left[s_{u1}(\tau) - s_{u1}(0)\right] + \cdots \tag{4.10}$$

and

$$z_{u0}(\tau) - h + \sigma z_{u1}(\tau) + \cdots$$

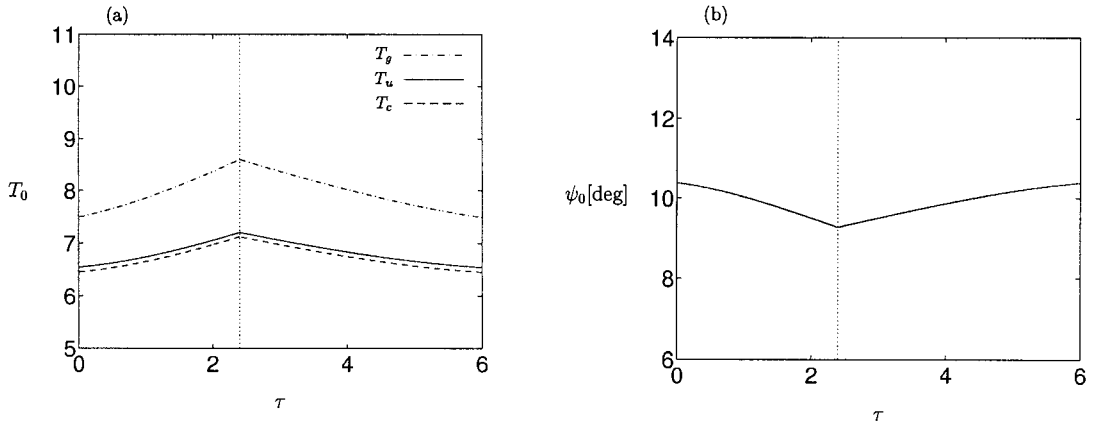

Figure 5. Variation of: (a) tension at distinguished points along the yarn, (b) angle the yarn tangent rotates through in the boundary layer. The parameter values are $V_c = 1$, $\mu = 0{\cdot}1$, $p_0 = 3{\cdot}0$, $h = 6$, $H = 3$, $|\phi_u| = 10^\circ$ and $\tau_1 = 2{\cdot}397$ (dotted line).

$$= \begin{cases} \tau|\Phi_u| + \sigma|\Phi_u|\,[s_{u0}(\tau) - s_{u0}(0)] + \cdots, & 0 \le \tau \le \tau_1 \\ 2H - \tau|\Phi_u| - \sigma|\Phi_u|\,[s_{u0}(\tau) - s_{u0}(0)] + \cdots. & \tau_1 \le \tau \le \sigma\Gamma \end{cases} \tag{4.11}$$

Note that the component $z_u(\tau)$ of $\mathbf{R}_u(\tau)$ and all of the quantities in Equation (4.9) are determined to $O(\sigma)$ solely by the $O(1)$ solution.

The leading order problem has now been reduced to solving a sequence of $O(1)$ equations: $\mathbf{R}_0' \cdot \mathbf{R}_0' = 1$ and

$$\mathbf{R}_0'' - 2\mathbf{k} \times \mathbf{R}_0' + \mathbf{k} \times (\mathbf{k} \times \mathbf{R}_0) = (T_0 \mathbf{R}_0')' + \mathbf{F}_0, \tag{4.12}$$

subject to the boundary conditions $\mathbf{R}_0(0) = \mathbf{0}$, continuity of $\mathbf{R}_0$, $\mathbf{R}_0'$ and T_0 at $s_{\ell 0}$, and the critical shear force condition

$$V_c = |[T_0(s_{u0}) - 1] \sin \psi_0|\,. \tag{4.13}$$

The slow time variable τ is now incremented and Equation (4.11) is used to obtain the corresponding value of $z_{u0}(\tau)$, which is used as a final boundary condition in the solution of the $O(1)$ equations as discussed in [3]. It should be noted that throughout the simulation, the concept of a 'virtual' package is assumed, where the lift-off point L never falls off the edge of the package. While this is an unrealistic physical assumption when the unwind point is moving near the front edge, it is adequate over most of the unwind cycle.

5. Numerical simulation

Figures 5 and 6 show results for the simulated unwinding of a package over a single unwind cycle with the guide-eye distance $h = 6$, package height $H = 3$, air drag coefficient $p_0 = 3$ and package surface friction $\mu = 0{\cdot}1$, for two values of critical shear force $V_c = 1$ and $V_c = 5$. The package wind-on angle is taken as $\phi_u = \pm 10^\circ$ so that $\sigma = 0{\cdot}1745$ and $|\Phi_u| = 1$. The asymmetry in the unwinding cycle is clearly visible with the period $\Gamma \sim 6$, where $\tau_1 \sim 2{\cdot}397$ for $V_c = 1$, and $\tau_1 \sim 2{\cdot}358$ for $V_c = 5$, as calculated from Equation (4.9). The values of τ_1 are marked in the figures by a vertical dotted line.

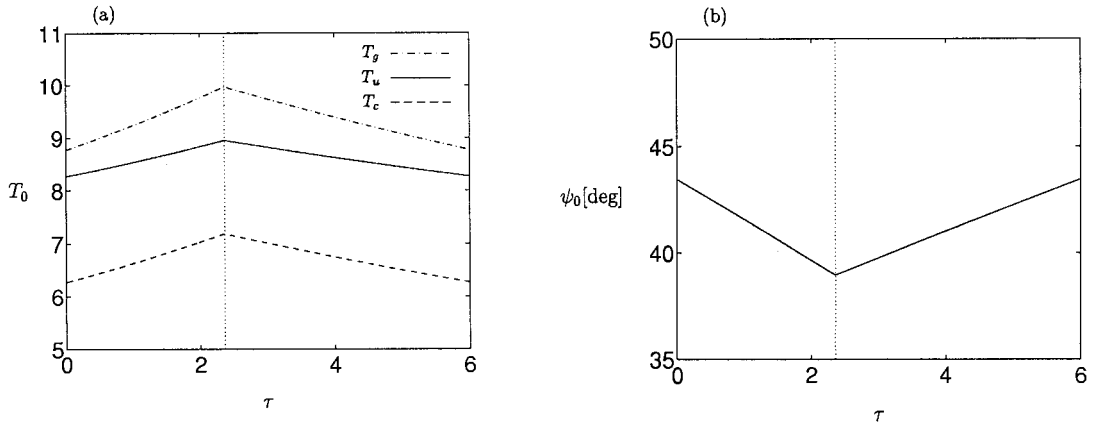

Figure 6. Variation of: (a) tension at distinguished points along the yarn, (b) angle the yarn tangent rotates through in the boundary layer. The parameter values are $Vc = 5$, $\mu = 0{\cdot}1$, $p_0 = 3{\cdot}0$, $h = 6$, $H = 3$, $|\phi_u| = 10^\circ$ and $\tau_1 = 2{\cdot}358$ (dotted line).

Figures 5a and 6a show yarn tension T_0 at three different locations: the guide eye $T_g = T_0(0, \tau)$ (dash-dot line); the asymptotic outer solution $T_u = T_0[s_{u0}(\tau)]$ (solid line); and the tension at the unwind point $T_c = \hat{T}_0(0, \tau)$ (dash line) which, by Equation (3.19), is

$$T_c = \hat{T}_0(0, \tau) = [T_0[s_{u0}(\tau)] - 1] \cos \psi_0 + 1.$$

The tension values at the guide eye T_g and the asymptotic outer solution tension T_u at the unwind point are much more sensitive to the value of V_c than is the tension in the boundary layer T_c at the unwind point. Over the unwinding of a package height $H = 3$, the tension at any of the three locations varies by about 10%.

Figures 5b and 6b show the variation of the angle ψ_0 through which the yarn tangent rotates in the bending boundary layer. ψ_0 is particularly sensitive to the value of V_c. In accordance with Equation (4.13), ψ_0 drops slightly as the unwind point approaches the far end of the package to compensate for the increased tension.

6. Concluding remarks

In this paper, a model of high speed package unwinding has been developed using the large deflection theory of elastic rods as applied to ring-spinning balloon dynamics in [10]. A singular perturbation analysis has been used to show that, over most of the yarn path between the guide eye and unwind point, the yarn behaves like a flexible string. Analysis of the boundary layer in the neighbourhood of the unwind point provides a model for the cohesive forces that hold the yarn winding in the package.

It has also been shown that the integration of the equation of motion for the unwind point is asymmetric in time, as observed experimentally, and that for small wind-on angle, the unwinding of a package can be simulated as a series of quasi-stationary unwinding balloons. This has extended the model developed in [3].

Acknowledgements

The research reported in this paper was supported by a grant from the U.S. National Textile Center through Clemson University to WBF, and by an Australian Research Council Large Grant to DMS and WBF. The authors thank Professor C.D. Rahn for his helpful discussions throughout the course of this work.

References

1. D.G. Padfield, The motion and tension in an unwinding balloon. *Proc. R. Soc. London* A245 (1958) 382–407.
2. V.K. Kothari and G.A.V. Leaf, The unwinding of yarn from packages. Parts I and II. *J. Text. Inst.* 70 (1979) 89–105.
3. W.B. Fraser, T.K. Ghosh and S.K. Batra, On unwinding yarn from a cylindrical package. *Proc. R. Soc. London* A436 (1992) 479–498.
4. W.B. Fraser, The effect of yarn elasticity on an unwinding balloon. *J. Text. Inst.* 83 (1992) 603–613.
5. W.B. Fraser, On the theory of ring spinning. *Phil. Trans. R. Soc. London* A342 (1993) 439–468.
6. .D. Clark, W.B. Fraser, R. Sharma and C.D. Rahn, The dynamic response of a ballooning yarn: theory and experiment. *Proc. R. Soc. London* A454 (1998) 2767–2789.
7. J. Kevorkian and J.D. Cole, *Multiple Scale and Singular Perturbation Methods.* Berlin: Springer-Verlag (1996) 632 pp.
8. X.M. Kong, C.D. Rahn and B.C. Goswami, Steady-state unwinding of yarn from cylindrical packages. *Textile Res. J.* 69 (1999) 292–306.
9. S.P. Timoshenko and J.M. Gere, *Mechanics of Materials.* (Third edition), London: Chapman & Hall (1987) 801 pp.
10. W.B. Fraser and D.M. Stump, Yarn twist in the ring-spinning balloon. *Proc. R. Soc. London* A454 (1998) 707–723.
11. A.E.H. Love, *A Treatise on the Mathematical Theory of Elasticity.* (Fourth edition). Cambridge: Cambridge University Press (1927) 643 pp.
12. D.M. Stump and W.B. Fraser, Bending boundary layers in moving strips. *Nonlinear Dynamics* 21 (2000) 55–70.